CFD Modeling and Simulation in Materials Processing 2018

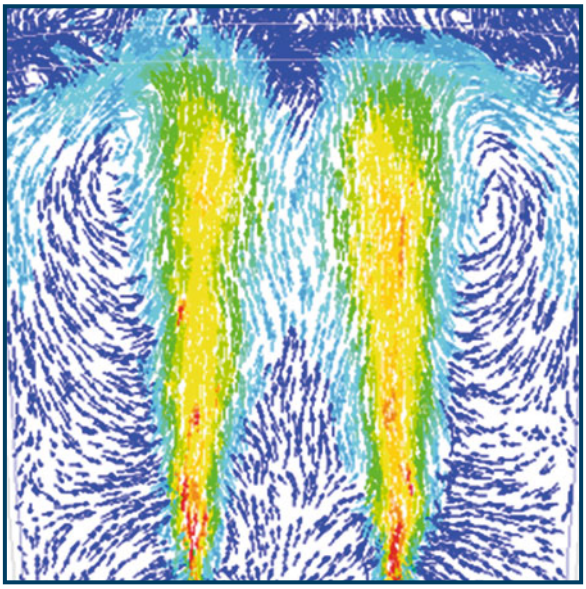

Edited by
Laurentiu Nastac, Koulis Pericleous,
Adrian S. Sabau, Lifeng Zhang,
and Brian G. Thomas

TMS

Springer

The Minerals, Metals & Materials Series

Laurentiu Nastac · Koulis Pericleous
Adrian S. Sabau · Lifeng Zhang
Brian G. Thomas
Editors

CFD Modeling and Simulation in Materials Processing 2018

TMS

Springer

Editors
Laurentiu Nastac
The University of Alabama
Tuscaloosa, AL
USA

Koulis Pericleous
University of Greenwich
London
UK

Adrian S. Sabau
Oak Ridge National Laboratory
Oak Ridge, TN
USA

Lifeng Zhang
University of Science and Technology Beijing
Beijing
China

Brian G. Thomas
Colorado School of Mines
Golden, CO
USA

ISSN 2367-1181 ISSN 2367-1696 (electronic)
The Minerals, Metals & Materials Series
ISBN 978-3-319-72058-6 ISBN 978-3-319-72059-3 (eBook)
https://doi.org/10.1007/978-3-319-72059-3

Library of Congress Control Number: 2017959908

Printed on acid-free paper

This Springer imprint is published by Springer Nature
The registered company is Springer International Publishing AG
The registered company address is: Gewerbestrasse 11, 6330 Cham, Switzerland

Preface

This book contains the proceedings of the symposium "CFD Modeling and Simulation in Materials Processing" held at the TMS 2018 Annual Meeting & Exhibition in Phoenix, Arizona, USA, March 11–15, 2018.

This symposium dealt with computational fluid dynamics (CFD) modeling and simulation of engineering processes. The papers published in this book were requested from researchers and engineers involved in the modeling of multiscale and multiphase phenomena in material processing systems.

The symposium focused on the CFD modeling and simulation of the following processes: Additive Manufacturing (Selective Laser Melting and Laser Powder Bed Fusion); Gas Atomization, Iron and Steelmaking (Continuous Casting, Blown Converter, Reheating Furnace, and Ladle Metallurgical Furnace); Submerged Arc Furnaces; Electrokinetic Deposition; Core Injection Molding; Evaporation of Metals; Friction Stir Welding; Ingot Casting; High Pressure Die Casting; and Casting and Solidification with Electromagnetic Field Interaction.

The symposium also covered applications of CFD to engineering processes and demonstrated how CFD can help scientists and engineers to better understand the fundamentals of engineering processes.

On behalf of all symposium organizers
and participants,
Laurentiu Nastac

Finite Element Modelling of Electrokinetic Deposition of Zinc on Mild Steel with ZnO-*Citrus sinensis* as Nano-Additive

Oluseyi O. Ajayi, Olasubomi F. Omowa, Oluwabunmi P. Abioye, Olugbenga A. Omotosho, Esther T. Akinlabi, Stephen A. Akinlabi, Abiodun A. Abioye, Felicia T. Owoeye and Sunday A. Afolalu

Abstract The electrokinetic deposition of zinc on mild steel substrate under the influence of ZnO-*Citrus sinensis* nano-additive was investigated numerically using a Finite Element (FE) solver. The conductivity of the Acid chloride plus ZnO-*Citrus sinensis* nano-additive electrolyte and the properties of Zinc and mild steel electrodes were used as the input codes for the model. The model was designed on a 3-dimensional scale. The boundary conditions were set and the model was meshed using the finer mesh capability in the FE solver. The model was processed and readings of the modelled zinc deposited mild steel were taken, validated and analysed so as to get the optimum parameters from the deposition process. Based on the results, the deposition mass and thickness increased with deposition time with ZnO-*Citrus sinensis* nano-additive, it is thus recommended that relatively high deposition time should be used in order to achieve optimum deposition.

Keywords Nano-additive · Nanotechnology · Corrosion protection Electrodeposition · Mild steel · Finite element · CFD

O. O. Ajayi (✉) · O. F. Omowa · O. P. Abioye · O. A. Omotosho · A. A. Abioye S. A. Afolalu
Department of Mechanical Engineering, Covenant University, Canaan Land, Ota, Ogun State, Nigeria
e-mail: oluseyi.ajayi@covenanatuniversity.edu.ng

E. T. Akinlabi
Department of Mechanical Engineering Science, University of Johannesburg, Johannesburg, South Africa

S. A. Akinlabi
Department of Mechanical and Industrial Engineering Technology, University of Johannesburg, Johannesburg, South Africa

F. T. Owoeye
Department of Chemistry, Covenant University, Canaan Land, Ota, Ogun State, Nigeria

L. Nastac et al. (eds.), *CFD Modeling and Simulation in Materials Processing 2018*, The Minerals, Metals & Materials Series,
https://doi.org/10.1007/978-3-319-72059-3_19

Introduction

Electrodeposition is a process of coating a thin layer of a metal on top of another metal so as to modify its surface properties. It helps in accomplishing the desired properties in a material. Such properties include the electrical and corrosion resistance, wear resistance, heat tolerance enhancement and decoration purposes [1, 2]. One of the ways to improve mild steel's value includes electrodeposition [3–5]. Electrokinetic deposition process is lately a process of interest to researchers because of its ability to enhance properties of different substrate materials such as mild steel at an affordable cost. Moreover, the phenomenon of electrodeposition comes by as a result of several experimentations which can be time consuming, repetitive, cost intensive and cumbersome, when there is the need to find optimum conditions. However, with the advent of computational fluid dynamics and finite element modelling/analysis, the process of simulating electrokinetic deposition becomes a cost-effective way to understand, optimize and control the electrodeposition processes.

Mild steel is an outstanding structural material. It is very affordable for engineering applications, can be easily formed and is mechanically strong. However, it rusts at low temperatures, and oxidises rapidly at high temperature [6]. Hence, there is a great need to improve the value of mild steel so that its intrinsic properties can be leveraged on and thus make the alloy more valuable in essential applications such as in our day to day lives and in industries which include the automotive, construction, electronics, electrical appliances, recreational and materials handling.

Relatively half of the world's consumption of zinc is used for the purpose of coating zinc on steel while electrodeposition of steel sheets consumes about 25–30% of the zinc produced [7, 8]. Zinc is appropriate to be utilised as a sacrificial cathode protector of steel from corrosion because its electronegativity of −0.6 V/standard hydrogen electrode (SHE) is over iron (Fe/Fe^{2+} 0.44 V/SHE) [9]. The exceptional resistive nature of zinc to corrosion is due to its ability to form adherent corrosion product films. Also, its corrosion rate is significantly lower than that of ferrous material (10–100 times depending on the environment). Additionally, zinc plating is fit to come in contact with edibles because zinc is nontoxic.

Acid chloride zinc plating is one of the most popular plating methods employed in developed countries. The first plating baths employed were acidic and zinc sulfate based. A great increase in the use of acid-zinc based bath has been noticed recently, as a result of environmental impact of cyanide-based bath which is toxic and expensive [10, 11].

The use of additives in aqueous electroplating solutions is really important because of its significant effects on the growth and structure of the deposits. Its benefits include enhancing mechanical and physical properties; brightening of the deposit, grain size reduction, stress and pitting reduction; increase in the current density range and stimulating levelling. However, the additives, which may be organic or metallic, ionic or non-ionic, are absorbed on the plated surface. For all

types of coating, the surface condition of the substrate is critical in terms of coating performance and durability [12].

A typical simulation produces the current distribution in the electrodeposition cell and at the electrodes' surface. The chosen FE solver is able to model cells when the thickness deposited is negligible compared to the inter-electrode gap and in event the growth and dissolution of the electrodes have to be considered using dynamic boundaries. Artificially modelling electrodeposition using for instance a Finite Element (FE) solver can help in the investigation of the influence of different parameters such as the time and additive concentration in the electrokinetic deposition process. This is the focus of this study. It additionally showed the ability to artificially model and analyse electrokinetic deposition of zinc on mild steel under the influence of organic zinc oxide-*Citrus sinensis* nanoadditive. It aimed to contribute to the very limited studies in this direction and employed a 3-D modelling procedure rather 2-D.

Materials and Methods

The modelling and simulation were carried out using a commercially available FE solver. The procedure follows three stages of pre-processing, processing and analysis, and post-processing.

Pre-processing

The FE model wizard was launched and a space dimension of 3-D was chosen. The electrodeposition module was used for the simulation. The geometry of the electrokinetic deposition setup was captured in the model. The model is as shown in Fig. 1.

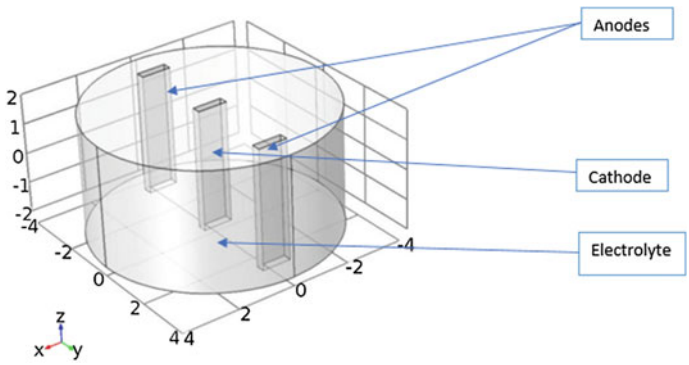

Fig. 1 The electrokinetic deposition setup model

Table 1 The geometry statistics of the model

Description	Value
Space dimension	3
Number of domains	1
Number of boundaries	18
Number of edges	48
Number of vertices	32

The electrokinetic deposition setup model consisted of the cathode, anodes and the container holding the electrolyte. The explicit selection node was created which allows for the boundary creation. The boundaries of the anodes and cathode were respectively defined, with boundaries 5–7, 11–13, 16, 18 for cathode and boundaries 8–10, 17 for the anode. The geometry statistics are defined as shown in Table 1.

Also, the combination of properties for the surface and the reaction stoichiometry which will determine how the magnitude and direction of the growth velocity of the deposited layer relate to the electrode reaction currents were defined. The external depositing electrode (i.e. the anode), surface properties and electrode reaction nodes were also defined (definitions are shown in Table 2).

Table 2 Parameters for the deposition model

Parameters	Value
Electrolyte conductivity (acid chloride + 1 Mol ZnO-*Citrus sinensis* nano-additive)	0.1964 S/m
Electrolyte conductivity (acid chloride only)	0.2013 S/m
Current	0.8 A
Cathode current density (mild steel)	0.020 A/m^2
Density of anode (Zinc)	7.13 g/mL
Density of cathode (Steel)	7.85 g/mL
Assumption	Model is isotropic
Equilibrium potential	0.7618 V
Temperature derivative of equilibrium potential	0 [V/K]
Kinetics expression type	Linearized butler—Volmer
Exchange current density	2.6e5 [A/m^2]
Molar mass of zinc	0.06538 kg/mol
Molar mass of steel	0.05584 kg/mol
Anodic transfer coefficient	0.5
Cathodic transfer coefficient	0.5
Active specific surface area	1e6 [1/m]
Limiting current density	Off
Number of participating electrons	2
Stoichiometric coefficient	1

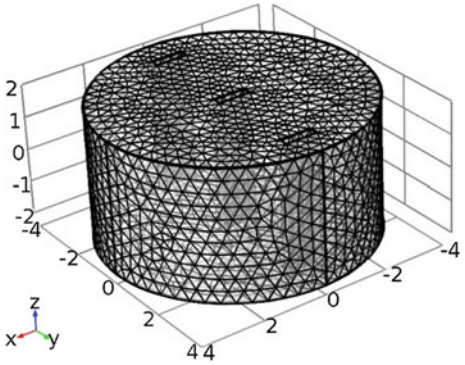

Fig. 2 Meshed electrokinetic deposition model

The cathode was defined to be mild steel, Anodes were made of pure zinc and the electrolyte initially used was acid chloride which was later changed to acid chloride + 1 Mol Zinc Oxide-*Citrus sinensis* nano-additive. The properties of the Cathode, Anode and electrolytes were thus captured as the input codes for the model as the model parameters (as shown in Table 2). Some of the parameters used for the model were measured while others were as obtained in the literature.

Meshing was done on the model using a physics-controlled mesh with finer mesh element size employed. The meshed model is shown in Fig. 2.

The simulation was set as time dependent and fixed geometry. The processing time was configured in seconds and in a range (0, 30, 1500).

Processing and Analysis

The simulation was computed by varying the deposition time with and without the ZnO-*Citrus sinensis* nano-additive. The FE solver then solved the problem at every node during the simulated deposition process.

The analysis was done by the FE solver as explained below.

The overpotential, μ_i, for an electrode reaction of index i, can be defined according to the following equation:

$$\mu_i = \beta_{m,0} - \beta_1 - X_{eq,i} \tag{1}$$

where $\beta_{m,0}$ denotes the electric potential of the metal, β_1 denotes the potential in the electrolyte, and $X_{eq,i}$ denotes the difference between the metal and electrolyte potentials at the electrode surface measured at equilibrium using a common reference potential. The electric potential of the metal at the anode is equal to the cell voltage. The potential of the electrolyte floats and adapts to satisfy the balance of current, so that an equal amount of current that leaves at the cathode also enters at the anode. This then determines the overpotential at the anode and the cathode.

The model used the electrodeposition and secondary interface to solve for the electrolyte potential, β_l (V), according to:

$$\begin{aligned} n_l &= -\alpha_l \Delta \beta_l \\ \Delta \cdot n_l &= 0 \end{aligned} \tag{2}$$

where n_l(A/m^2) is the electrolyte current density vector and α_l (S/m) is the electrolyte conductivity, which is assumed to be a constant. Using the default Insulation condition for all boundaries excluding the anode and cathode surfaces:

$$p \cdot n_l = 0 \tag{3}$$

as p is the normal vector, pointing out of the domain. The main electrode reaction on both the anode and the cathode surfaces is the zinc deposition/dissolution reaction given as:

$$\mathrm{Zn}^{2+} + 2\mathrm{e}^- \leftrightarrow \mathrm{Zn}(s) \tag{4}$$

Using the Butler-Volmer expression to model this reaction, this will set the local current density to:

$$n_{loc,\mathrm{Zn}} = n_{0,\mathrm{Zn}} \left(\exp\left(\frac{\varepsilon_a F \mu_{Zn}}{RT} \right) - \exp\left(\frac{\varepsilon_c F \mu_{Zn}}{RT} \right) \right) \tag{5}$$

The rate of deposition at the cathode boundary surfaces and the rate of dissolution at the anode boundary surface, with a velocity in the normal direction, v (m/s), can be calculated according to:

$$V = \frac{n_{loc,\mathrm{Zn}}}{pF} \frac{M}{\rho} \tag{6}$$

where M is the mean molar mass (65 g/mol) and ρ is the density (7130 kg/m^3) of the Zinc atoms and p is number of participating electrons. It should be noted that the local current density is positive at the anode and negative at the cathode surfaces. On the anode the electrolyte current density is set to the local current density of the zinc deposition reaction:

$$p \cdot n_l = n_{loc,\mathrm{Zn}} \tag{7}$$

On the cathode, a second electrode reaction was added to model the parasitic hydrogen evolution reaction:

$$2\mathrm{H}^+ + 2\mathrm{e}^- \leftrightarrow \mathrm{H}_2 \tag{8}$$

A cathodic Tafel equation was used to model the kinetics of the hydrogen reaction on the cathode, this will thus set the local current density to:

$$n_{loc,\mathrm{H}} = -n_{o,\mathrm{H}} 10^{-\mu/A} \tag{9}$$

The hydrogen reaction will not affect the rate of deposition of zinc, but it will affect the total current density at the cathode surface:

$$p \cdot n_l = n_{loc,\mathrm{Zn}} + n_{loc,\mathrm{H}} \tag{10}$$

Thus, simulating the deposition with time dependent and fixed geometry,

$$n_1 \cdot p = n_{total} \tag{11}$$

$$n_{total} = \sum_i n_{loc \cdot i} + n_{dl} \tag{12}$$

$$\frac{\partial C_{m,n}}{\partial t} + \Delta_t \cdot \left(-D_n \Delta_t c_{m,n}\right) = R_{m,n} \tag{13}$$

$$N_{m,n} = -D_n \Delta_t c_{m,n} \tag{14}$$

$$\emptyset_n = \frac{c_{m,n} \alpha_n}{\neg_s} \tag{15}$$

$$\frac{\partial c_{dep,n}}{\partial t} = R_{dep \cdot n} \tag{16}$$

$$p \cdot \frac{\partial x}{\partial t} = \sum_n \frac{R_{dep,n} M_n}{\rho_n} \tag{17}$$

$$\Delta \cdot n_l = Q_i \tag{18}$$

$$n_1 = -\alpha_1 \Delta \beta_1 \tag{19}$$

Also with:

$$\Delta \cdot n_m = Q_m \tag{20}$$

$$n_m = -\alpha_m \Delta \beta_m \tag{21}$$

where,

β_1 = phil and β_m = phis; phil is the electrolyte potential and phis is the electric potential.

Post-processing

The solution data set was added, the surface plot was created to get the thickness and mass change of the electrodes and the second surface plot for current efficiency was created. Likewise, the thickness and mass changes were captured when the electrolyte conductivity is updated with the addition of 1 Mol ZnO-*Citrus sinensis* nano-additive data.

Results and Discussion

Electrolyte Potential

Figure 3 shows the potential of the electrolyte during deposition. Based on the simulation, the electrolyte has the lowest value of potential around the cathode and highest value of potential around the anodes.

Anode Electrode Change

The anode's thickness and mass reduced significantly as shown in the simulation in Fig. 4. Also, Fig. 5a, b shows that the anode electrodes thickness and mass consistently decreased with time. The anode reduced by about 2.1×10^{-6} m in thickness and 0.0145 kg/m^3 after depositing for 1500 s.

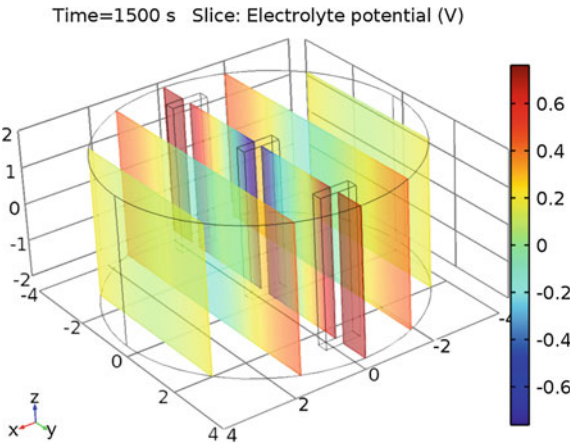

Fig. 3 Potential of the electrolyte during deposition

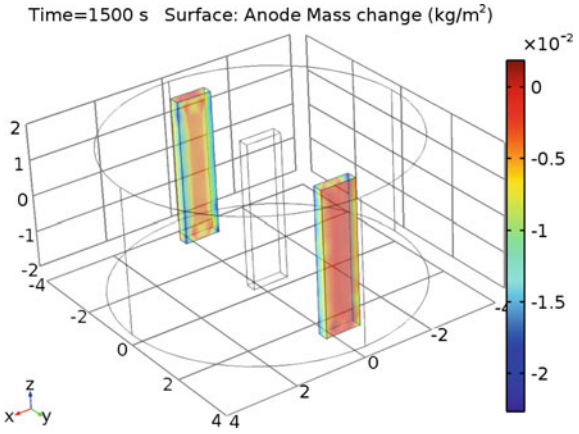

Fig. 4 Surface: anode mass change (kg/m^2) at the end of deposition

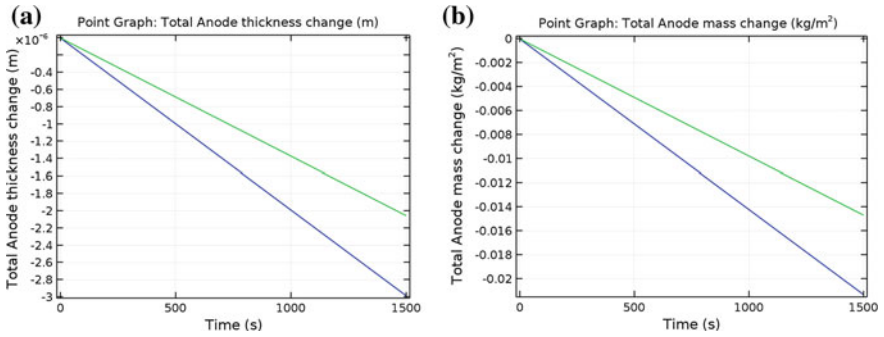

Fig. 5 Point graph, **a** Total anode thickness change (m), **b** Total anode mass change (kg/m^2)

Cathode Electrode Change

At the end of the deposition, significant increase in mass was observed in the cathode, this confirms that the deposition process led to a mass increase in the cathode as shown in Fig. 6. Also, Fig. 7a, b shows that the cathode electrode thickness and mass consistently increased with time. The cathode increased by about 2.2×10^{-6} m in thickness and 0.017 kg/m^3 in mass after depositing for 1500 s.

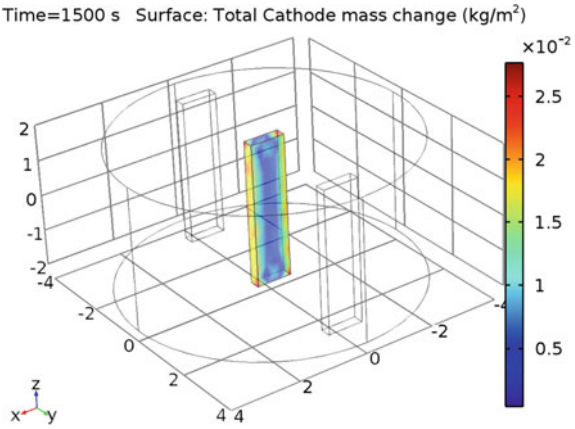

Fig. 6 Surface: Total Cathode mass change (kg/m^2) at the end of deposition

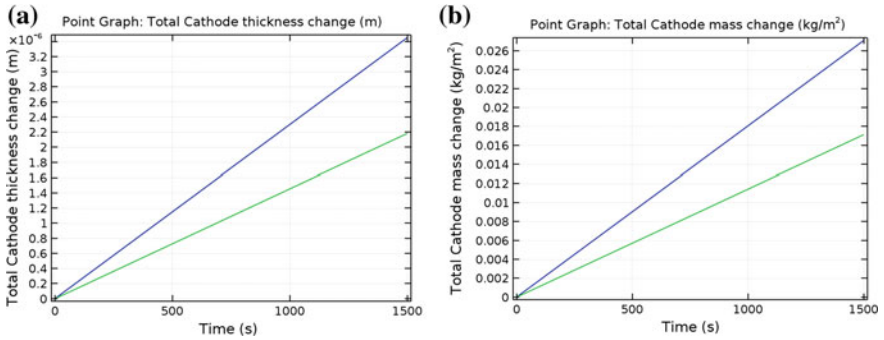

Fig. 7 Point graph, **a** Total cathode thickness change (m), **b** Total cathode mass change (kg/m^2)

Comparison of the Results of Cathode Change from the FE Solver with Experimentation

Figure 8 shows the result of the cathode mass change, the same mass change trend was observed both in the simulated result (shown in Fig. 7b) and experimental result. The experimental result shows the actual mass change from the deposition while the simulated result shows the expected result in an ideal situation (thus the reason for the slight deviation seen between 600 and 900 s in the experimental result's graph). This mass change trend in the experimental result validates the accuracy of the simulation.

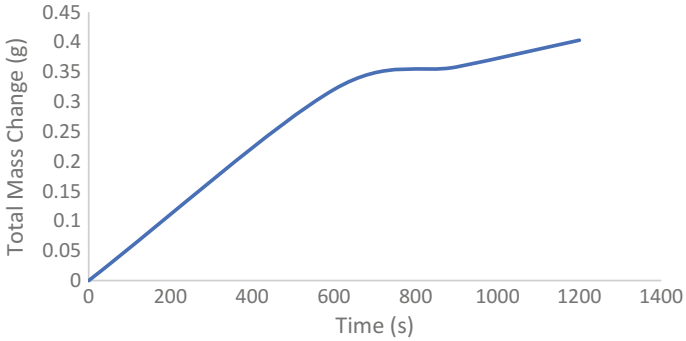

Fig. 8 Experimental result of the cathode mass change

*Effect of ZnO-*Citrus sinensis *Nano-Additive on the Electrokinetic Deposition*

To get the effect of ZnO-*Citrus sinensis* nano-additive on the electrokinetic deposition, the data of the electroconductivity in the model was updated with the data for 1 Mol of ZnO-*Citrus sinensis* nano-additive (as stated in Table 2). Figure 9 shows the result showing the impact of the 1 Mol ZnO-*Citrus sinensis* nano-additive on the cathode thickness and mass changes.

Without the additive, the cathode increased by about 2.2×10^{-6} m in thickness and 0.017 kg/m^3 in mass after depositing for 1500 s; while with 1 Mol ZnO-*Citrus sinensis* nano-additive, the cathode increased by about 2.18×10^{-6} m in thickness and approximately 0.017 kg/m^3 after depositing for 1500 s. Based on the results from the simulation, the impact of 1 Mol of the nanoadditive used is insignificant in electrokinetic deposition of zinc on mild steel in acid chloride environment. Similar results were also gotten at the anodes when comparing with and without the 1 Mol ZnO-*Citrus sinensis* nano-additive (i.e. The anode reduced by about 2.1×10^{-6} m in thickness and 0.0145 kg/m^3 after depositing for 1500 s).

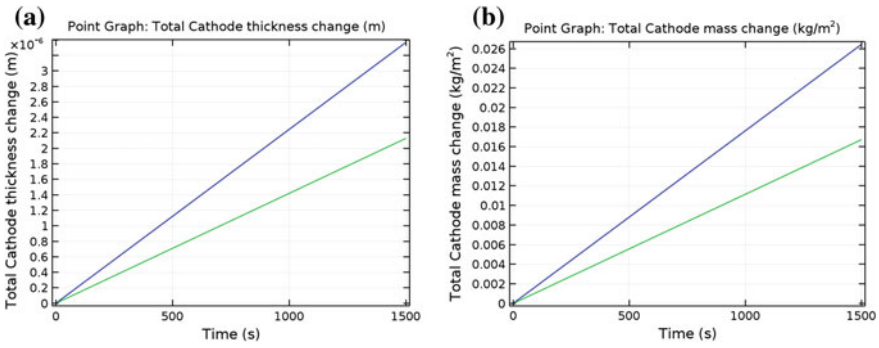

Fig. 9 Point graph, **a** Total cathode thickness change (m), **b** total cathode mass change (kg/m^2)

Although physical examination of the zinc deposited mild steel shows a smoother surface finish when ZnO-*Citrus sinensis* as nano-additive was included in the electrolyte solution, the simulation and experiment showed an insignificant impact of the nano-additive on mass and thickness changes in the deposition.

Conclusion

The electrokinetic deposition of zinc on mild steel with ZnO-*Citrus sinensis* as nano-additive was artificially studied using a commercially available FE solver. With and without the ZnO-*Citrus sinensis* nano-additive, the Cathode's thickness and mass increased while the Anode's thickness and mass reduced with the deposition time. The amount of mass and thickness increment in the Cathode is similar to the total amount of mass and thickness reduction in the anodes. Thus, high deposition time is required for optimum deposition. This study showed that electrokinetic deposition aid consistent mass exchange between the cathode and anode, thus it is an efficient and effective deposition method. Also, there was no significant impact of the ZnO-*Citrus sinensis* nano-additive on the mass and thickness changes in the anodes and cathode from the simulation and experiment despite a smoother surface achieved with ZnO-*Citrus sinensis* nano-additive when examined physically.

It also shows that the process can effectively be investigated artificially without recourse to experimentation.

References

1. Bruce KG (2012) Electro chemical deposition: principles, methods and applications
2. Schlesinger M, Paunovic M (eds) (2000) Modern electroplating, 4th ed. Wiley, New York
3. Loto CA, Olefjord I (1992) Corr Prev Control J 39:142–149
4. Loto CA, Olefjord I (1990) Corr Prev Control J 37(5):158–163
5. Loto CA., Olefjord I, Mattson H (1992) Corros Prev Control J 39:82–88
6. Ashby MF, Jones DRH (2002) Engineering materials 1. An introduction to their properties and applications. Second Edition. Department of Engineering, University of Cambridge, UK. ISBN 0 7506 3081 7, pp 211–232
7. Asamura T (1998) Proceedings of the 4th international conference on zinc and zinc alloy coated steel sheet. Galvatech '98, Chiba, Japan. The iron and steel institute of Japan, pp 14–21
8. Goodwin FE (1998) Proceedings of the 4th international conference on xinc and zinc alloy coated steel sheet. Galvatech '98, Chiba, Japan. The iron and steel institute of Japan, pp 31–39
9. Winand R (2010) Electrodeposition of zinc and zinc alloys. Wiley, USA. pp 285–307
10. Loto CA (2012) Influence of *Ananas comosus* juice extract as additive on the electrodeposition of zinc on mild steel in acid chloride solution. Int J Electrochem Sci 7:10748–10762

11. Loto CA, Olofinjana A, Popoola API (2012) Effect of *Saccharum officinarum* juice extract additive on the electrodeposition of zinc on mild steel in acid chloride solution. Int J Electrochem Sci 7:9795–9811
12. Park DY, Myung NV, Schwartz M, Nobe K (2002) Electrochim Acta 47:2893–2900